

1 **Short Title:** Variation in C<sub>4</sub> pathways in maize growth  
2

3 **Authors for Contact:** Jennifer J. Arp, [jarp@danforthcenter.org](mailto:jarp@danforthcenter.org); Doug K. Allen,  
4 [doug.allen@usda.gov](mailto:doug.allen@usda.gov)  
5

6 **Developmental Effects on Relative Use of PEPCK and NADP-ME Pathways of C<sub>4</sub>**  
7 **Photosynthesis in Maize**  
8

9 Jennifer J. Arp<sup>1</sup>, Shrikaar Kambhampati<sup>1</sup>, Kevin L. Chu<sup>1</sup>, Somnath Koley<sup>1</sup>, Lauren M. Jenkins<sup>1,2</sup>,  
10 Todd C. Mockler<sup>1</sup>, and Doug K. Allen<sup>1,2</sup>.  
11

12 (1) Donald Danforth Plant Science Center, Saint Louis, MO 63132 USA

13 (2) United States Department of Agriculture, Agricultural Research Service, Saint Louis, MO  
14 63132 USA  
15

16 **One Sentence Summary:** The proportion of the two C<sub>4</sub> pathways in maize plants is dependent  
17 on canopy position and not the age of the leaf.  
18

19 **Author Contributions:** J.A. and D.K.A. conceived the research plans; S.Ka., S.Ko., K.C.,  
20 L.J., and J.A. performed labeling and metabolite quantitation experiments; J.A.  
21 designed the experiments and analyzed the data; J.A. wrote the article with  
22 contributions of all the authors; D.K.A. supervised and completed the writing. D.K.A.  
23 agrees to serve as the author responsible for contact and ensures communication.  
24

25 **Responsibilities of the Author for Contact:** It is the responsibility of the author for contact to  
26 ensure that all scientists who have contributed substantially to the conception, design or  
27 execution of the work described in the manuscript are included as authors, in accordance with  
28 the guidelines from the Committee on Publication Ethics (COPE)  
29 (<http://publicationethics.org/resources/guidelines>). It is the responsibility of the author for contact  
30 also to ensure that all authors agree to the list of authors and the identified contributions of  
31 those authors.  
32

33 **Funding Sources:** Funding for the research was provided by the National Science Foundation  
34 Plant Genome Research Program (PGRP) postdoctoral fellowship (NSF-1812235) to J.A., and  
35 PGRP Award IOS-1829365, the United States Department of Agriculture National Institute of  
36 Food and Agriculture (2017-67013-26156; 2016-67013-24585), the Office of Biological and  
37 Environmental Research in the DOE Office of Science (DE-SC0008769), and the National  
38 Institutes of Health (U01 CA235508). Support was also provided by United States Department  
39 of Agriculture Agricultural Research Service. Support for the acquisition of the 6500 QTRAP  
40 LC-MS/MS was provided by the National Science Foundation (DBI #1427621).  
41  
42

43 **Abstract**

44

45 C<sub>4</sub> photosynthesis is an adaptive photosynthetic pathway which concentrates CO<sub>2</sub> around  
46 Rubisco in specialized bundle sheath cells to reduce photorespiration. Historically, the pathway  
47 has been characterized into three different subtypes based on the decarboxylase involved,  
48 although recent work has provided evidence that some plants can use multiple decarboxylases,  
49 with maize in particular using both the NADP-malic enzyme (NADP-ME) pathway and  
50 phosphoenolpyruvate carboxykinase (PEPCK) pathway. Parallel C<sub>4</sub> pathways could be  
51 advantageous in balancing energy and reducing equivalents between bundle sheath and  
52 mesophyll cells, in decreasing the size of the metabolite gradients between cells and may better  
53 accommodate changing environmental conditions or source to sink demands on growth. The  
54 enzyme activity of C<sub>4</sub> decarboxylases can fluctuate with different stages of leaf development,  
55 but it remains unclear if the pathway flexibility is an innate aspect of leaf development or an  
56 adaptation to the leaf microenvironment that is regulated by the plant. In this study, variation in  
57 the two C<sub>4</sub> pathways in maize were characterized at nine plant ages throughout the life cycle.  
58 Two positions in the canopy were examined for variation in physiology, gene expression,  
59 metabolite concentration, and enzyme activity, with particular interest in asparagine as a  
60 potential regulator of C<sub>4</sub> decarboxylase activity. Variation in C<sub>4</sub> and C<sub>3</sub> metabolism was observed  
61 for both leaf age and canopy position, reflecting the ability of C<sub>4</sub> pathways to adapt to changing  
62 microenvironments.

## 63 Introduction

64  
65 C<sub>4</sub> photosynthesis is a beneficial adaptation to environmental conditions that enables plants to  
66 more effectively assimilate carbon dioxide relative to C<sub>3</sub> plants, resulting in some of the most  
67 productive crops on a biomass basis. C<sub>4</sub> photosynthesis has evolved over 60 times in plants to  
68 overcome the inefficiencies of Rubisco by minimizing the oxidation reaction and  
69 photorespiration (Sage et al., 2011). The pathway has historically been categorized into three  
70 subtypes based on the decarboxylase—NAD-malic enzyme (NAD-ME), NADP-malic enzyme  
71 (NADP-ME) or phospho~~eno~~pyruvate carboxykinase (PEPCK)—but additional evidence has  
72 identified plants that can use a combination of decarboxylases in C<sub>4</sub> photosynthesis (Chapman  
73 and Hatch, 1981; Furbank, 2011; Wang et al., 2014). Several advantages of using a  
74 combination of C<sub>4</sub> pathways have been proposed. By dividing the transfer of metabolites  
75 between the mesophyll and bundle sheath into a combination of amino and organic acids,  
76 smaller gradients of each are sufficient to drive the transfer between cell types (Pick et al., 2011;  
77 Stitt and Zhu, 2014; Wang et al., 2014). The two pathways distribute energy and reducing  
78 equivalents differently between the two cell types which could be complementary and provide  
79 faster response to shifting light environments (Furbank, 2011; Stitt and Zhu, 2014). The ratio of  
80 NADP-ME to PEPCK pathway flux may not be fixed within species, across plant development,  
81 or under changing environment. Literature reports in maize indicate PEPCK flux is 10-25% of  
82 total C<sub>4</sub> flux (Chapman and Hatch, 1981; Weissmann et al., 2016; Arrivault et al., 2017),  
83 whereas in the C<sub>4</sub> dicot *Flaveria bidentis*, 50% of assimilated carbon comes through the PEPCK  
84 pathway (Meister et al., 1996). More broadly, enzyme activities for key C<sub>4</sub> enzymes in NADP-  
85 ME-type species also indicate extensive variation in the ratio of aspartate to malate translocated  
86 in C<sub>4</sub> plants (Kanai and Edwards, 1999). The ratio of malate and aspartate can also fluctuate in  
87 response to nitrogen limitation (Khamis et al., 1992). Though multiple studies have observed  
88 differences in pathway flux, the factors that elicit particular C<sub>4</sub> photosynthetic subtype use  
89 remain to be firmly established and could aid efforts to sustainably increase crop productivity.

90  
91 The role for dual C<sub>4</sub> pathways has been considered over plant development in *Cleome gyandra*  
92 (Sommer et al., 2012). In this dicot species, decarboxylase activity varied with leaf age along  
93 the canopy using the NAD-malic enzyme pathway and a supplemental PEPCK pathway. In  
94 younger leaves, the activity of NAD-ME was twice that of PEPCK; however, in older leaves,  
95 PEPCK activity increased and NAD-ME activity decreased, leading to nearly double PEPCK  
96 activity compared to NAD-ME while the total amount of decarboxylase activity remained nearly  
97 constant. Though the study was intended to characterize the establishment of C<sub>4</sub>

98 photosynthesis across development, the findings established within-plant differences and  
99 indicated the ratio of pathway use is pliable within species.

100

101 Canopy position and the resulting light environment of the leaf has an effect on the rate of  
102 photosynthesis. In the maize canopy, all new leaves form in full sunlight at the top of the canopy  
103 and become progressively shaded by new growth, requiring leaves to adapt to the new  
104 environment after they are fully formed. In the maize canopy, the gradients of light and age  
105 generate a pattern of increasing photosynthetic capacity at the top of the canopy, and less  
106 activity at the bottom of the canopy from older, self-shaded leaves (Ubierna et al., 2013;  
107 Niinemets, 2016; Pons, 2016; Collison et al., 2020). Up to 50% of maize photosynthesis occurs  
108 in these shaded parts of the canopy (Baker et al., 1988), and leaves in the lower canopy are  
109 capable of high rates of photosynthesis when not exposed to large degrees of self-shading  
110 (Collison et al., 2020). In addition to differences in overall rates of photosynthesis, foundational  
111 work on light regulation in maize has shown that the C<sub>4</sub> enzymes are more light-controlled than  
112 the C<sub>3</sub> enzymes (Sugiyama et al., 1984; Ward and Woolhouse, 1986). However, at low light,  
113 the C<sub>3</sub> pathways are expected to be more downregulated than C<sub>4</sub> as the plant shifts N away  
114 from Rubisco and toward light harvesting (Boardman, 1977; Björkman, 1981; Hikosaka and  
115 Terashima, 1995; Evans and Poorter, 2001; Walters, 2005; Tazoe et al., 2006; Pengelly et al.,  
116 2010). Moreover, species utilizing different C<sub>4</sub> subtypes have different degrees of shade  
117 acclimation, with C<sub>4</sub> grasses which use the NADP-ME subtype, such as *Z. mays*, able to  
118 acclimate to shade more readily than those using NAD-ME or PEP-CK subtypes (Sonawane et  
119 al., 2018).

120

121 The interaction between C<sub>4</sub> pathways and plant nitrogen status is well-documented (Khamis et  
122 al., 1992; Taub and Lerda, 2000; Ghannoum et al., 2005; Pinto et al., 2014; Pinto et al., 2016)  
123 but mechanistically is not completely understood. The PEPCK pathway shuttles carbon using  
124 the amino acid aspartate which provides a potential regulatory link between C<sub>4</sub> photosynthesis  
125 and the nitrogen status of the plant. Aspartate can be rapidly converted to asparagine that is  
126 associated with important developmental cues during the maize life cycle (Seebauer et al.,  
127 2004) and transports carbon and nitrogen between leaves and developing kernels (Cañas et al.,  
128 2010). Asparagine is believed to play a role in signaling seed storage protein deposition  
129 (Hernández-Sebastià et al., 2005; Pandurangan et al., 2012) and, importantly, appears to be a  
130 regulator of PEPCK activity in seeds. When asparagine was added exogenously to grape  
131 seeds, PEPCK activity was increased 100-fold (Walker et al., 1997). This relationship is likely

132 important *in vivo* because PEPCK proteins are developmentally regulated in tomato and grape  
133 seeds (Walker et al., 1999; Bahrami et al., 2001), and PEPCK activity coincides with peak  
134 amino acid metabolism and storage protein deposition, possibly through asparaginase activity  
135 (Walker et al., 1999). Despite known anaplerotic functional relationships between asparagine  
136 and PEPCK, it remains unclear if asparagine could be important for the regulation of the C<sub>4</sub>  
137 PEPCK gene during development and aging of the maize leaf.

138

139 In this study, we grew maize plants at ten day intervals to sample leaves from the top and  
140 middle of the canopy at nine plant ages to determine the effect of canopy position and plant age  
141 on the proportion of C<sub>4</sub> flux through PEPCK relative to NADP-ME. Parts of the canopy with the  
142 greatest fluctuations in light environment, including lower leaves, would be expected to use  
143 proportionally more mixed C<sub>4</sub> pathways to allow leaf cells to maintain an energetic homeostasis.  
144 Additionally, plant age might affect the C<sub>4</sub> pathways such that older plants would use  
145 proportionately more equal C<sub>4</sub> pathways to maintain moderate levels of photosynthesis as leaf N  
146 is remobilized to the grain during senescence. One possible regulator of PEPCK variation based  
147 on work in other species is asparagine, so asparagine concentration across development was  
148 compared with C<sub>4</sub> pathway activity to identify potential regulatory relationships. Overall, we  
149 found the plant modifies the proportion of the two C<sub>4</sub> photosynthetic pathways in response to the  
150 developmental and environmental microenvironment of the leaf throughout the growing season.

## 151 **Results**

### 152 *Distinguishing maize plant developmental progression from canopy influence*

153 To understand variation in the C<sub>4</sub> pathways over the course of the plant life cycle and within the  
154 canopy, maize plants (*var.* W22) were grown in ten-day intervals for 100 days in the greenhouse  
155 from February to July 2019. Plants were sampled on July 2-3, 2019, for the nine developmental  
156 times, representing plants 15 days after sowing to 100 days after sowing (DAS; Figure 1).  
157 Measurements were taken from the top collared leaf (“top leaf”) and leaf 13 (“subtending leaf”),  
158 which is the leaf subtending the ear in W22. All measurements were taken from the middle of  
159 the leaf, 20 cm from the leaf tip. The top leaf represents the leaf receiving the highest amount of  
160 sunlight and is the youngest expanded leaf on the maize plant. The subtending leaf provides the  
161 most nutrients to support ear growth (Subedi and Ma, 2005). Measurements were not taken  
162 from leaves within the whorl nor from leaves which had fully senesced. In total, these leaf

163 samples represented the span of the maize life cycle and two functionally distinct parts of the  
164 leaf canopy.

165

#### 166 *Photosynthetic CO<sub>2</sub> assimilation decreased with plant age*

167 Overall photosynthetic rate has been shown to be variable during plant growth and in the  
168 canopy (Dwyer and Stewart, 1986; Chen et al., 2016; Niinemets, 2016), so we measured net  
169 CO<sub>2</sub> assimilation ( $A_{net}$ ) on the plants at the nine growth stages.  $A_{net}$  was measured at both  
170 ambient (350  $\mu\text{mol m}^{-2} \text{s}^{-1}$ ) and high (1500  $\mu\text{mol m}^{-2} \text{s}^{-1}$ ) light levels in the LI-6800 chamber.  
171 During plant growth  $A_{net}$  consistently decreased with age in the plant for both top and  
172 subtending leaves at the ambient and high light levels (Figure 2A). Leaf position did not have a  
173 significant effect on  $A_{net}$  ( $p=0.90$ , ANOVA type II). The interaction between light and plant age  
174 was significant ( $p=5.96\text{e-}6$ , ANOVA): in young plants,  $A_{net}$  increased substantially in the high  
175 light conditions compared to 500  $\mu\text{mol m}^{-2} \text{s}^{-1}$ ; however, the response to high light was  
176 dampened in older plants.

177

#### 178 *Chlorophyll content and $A_{net}$ are correlated with plant age*

179  $A_{net}$  was modestly correlated with chlorophyll concentration in the leaf (Pearson's  $R = 0.39$ ) as  
180 an overall indicator of photosynthetic capacity. Total chlorophyll concentration increased in the  
181 top leaf from 0.6 mg chlorophyll  $\text{g}^{-1}$  FW to 1.1 mg  $\text{g}^{-1}$  FW between 15 DAS and 60 DAS before  
182 decreasing back to 0.6 mg  $\text{g}^{-1}$  FW at 80DAS, the last sampling time for the top leaf before  
183 complete senescence (Figure 2B). Leaf position in the canopy did not have a significant effect  
184 on total chlorophyll concentration ( $p=0.12$ , ANOVA type II); however, plant age had a significant  
185 effect ( $p=0.004$ ). Chlorophyll concentration decreased steadily in the subtending leaf, likely as a  
186 consequence of the initiation of leaf senescence (Figure 2B). Throughout the growth cycle, the  
187 nitrogen status of the leaf and the light environment are expected to vary and can affect the  
188 chlorophyll a to b ratio (Hikosaka and Terashima, 1995). Chlorophyll a to b ratio was not  
189 correlated with the age of the plant or canopy position ( $p=0.14$  and  $p=0.73$ , ANOVA type II);  
190 however, the interaction effect between leaf position and plant age was significant ( $p=0.001$ ,  
191 ANOVA type II; Figure 2C), and the ratio drops slightly in the top leaves at 70 and 80 days after  
192 sowing, reflecting the beginning of senescence.

193

194 *Ratio of C<sub>4</sub> decarboxylases changed with canopy position and plant age*

195 The responses of the two C<sub>4</sub> pathway decarboxylases were investigated using transcriptional  
196 analysis since the enzymes involved in the C<sub>4</sub> pathway are at least partially regulated at this  
197 level (Pick et al., 2011). Using the gene expression atlas resource for maize (Stelpflug et al.,  
198 2016), gene expression levels were probed for the two decarboxylase enzymes in maize leaves  
199 over developmental age. Both PEPCK1 (GRMZM2G001696) and NADP-ME (NADP-ME3,  
200 GRMZM2G085019) expression varied with growth stage, beginning with the highest expression  
201 in the youngest leaves and decreasing with leaf age. NADP-ME3 expression decreased quickly  
202 after the V9 growth stage; its expression was approximately 2-fold higher than PEPCK1 until the  
203 V9 growth stage, where expression became approximately equal for the two decarboxylases  
204 (Figure 3A). Based on the transcriptomic evaluation, a comprehensive experiment was  
205 designed to assess the C<sub>4</sub> subtypes through the lifetime of leaves.

206

207 The expression of NADP-ME3 and PEPCK1 in the plants grown in the greenhouse was  
208 assessed by quantitative real-time PCR to confirm the trend indicated by the maize atlas.  
209 Similar to the pattern from the maize expression atlas, both C<sub>4</sub> decarboxylase genes decreased  
210 in relative expression as the leaf aged (Figure 3B). For both genes, expression was highest in  
211 the youngest leaf tissues and decreased continually in older leaves; the trend held for both the  
212 leaf at the top of the canopy and the leaf subtending the ear (Figure 3B). On average, NADP-  
213 ME3 was expressed at a level 2.4 times higher than PEPCK1. Unlike in the gene expression  
214 atlas, PEPCK1 expression was less divergent from NADP-ME3 expression in the youngest  
215 leaves, and more divergent in older leaves. Leaf position significantly impacted the expression  
216 of both NADP-ME3 and PEPCK1 expression, but not the ratio between the two genes.

217

218 Decarboxylase activity was also measured using enzyme activity assays. Maize plants exhibited  
219 variation in both the amount of enzyme activity and the ratio of NADP-ME to PEPCK activity  
220 depending on both canopy position of the leaf and growth stage of individual leaves (ANOVA  
221 activity ~ leaf \* plant age,  $p < 0.05$ ). Both enzyme activities in the top leaf were not significantly  
222 different with plant age. Canopy position had a large effect, with leaves in the top of the canopy  
223 exhibiting 35.7% more PEPCK and 62.2% more NADP-ME activity in the four growth stages  
224 where both leaves were measured (Figure 4). In the top of the canopy, NADP-ME activity was  
225 2-fold higher than PEPCK on average; however, in the subtending leaves, the ratio decreased  
226 to 1.5-fold higher, indicating a decreased relative role for NADP-ME in that part of the canopy.  
227 Thus, in the top leaves, 66% of decarboxylase activity came from NADP-ME and 34% from

228 PEPCK, while in the subtending leaves, the proportion shifted to 60% from NADP-ME and 40%  
229 from PEPCK.

230

231

### 232 *Pool sizes of C<sub>4</sub> and C<sub>3</sub> metabolites*

233 Malate and aspartate are the transfer acids that move CO<sub>2</sub> from the mesophyll to the bundle  
234 sheath. Concentrations of both metabolites were measured in the two leaves for nine growth  
235 stages with LC-MS/MS. In the 15-day old plants, the ratio of malate to aspartate was 4.6:1,  
236 similar to reported values (Chapman and Hatch, 1981; Weissmann et al., 2016; Arrivault et al.,  
237 2017) and with expected pool sizes: 6.5±1.4 μmol malate g<sup>-1</sup> FW and 1.4±0.6 μmol aspartate g<sup>-1</sup>  
238 FW (Khamis et al., 1992; Lohaus et al., 1998; Szecowka et al., 2013; Arrivault et al., 2017). Both  
239 plant age and canopy position had significant effects on the pool sizes of malate and aspartate  
240 (ANOVA, type II, p<0.0001; Figure 5). In the top leaf, the pool size of malate decreased from  
241 6.5±1.4 μmol g<sup>-1</sup> FW at 15 days to 2.2±0.8 μmol g<sup>-1</sup> FW for 30-80 DAS, while the aspartate pool  
242 size was largely unchanged with time. Thus, the ratio between the malate and aspartate pools  
243 decreased to 1.8±0.4 in the top leaf from 30 to 80 DAS (Figure 5). In the subtending leaf, the  
244 concentration of malate was generally greater than in the top leaf and both pool sizes  
245 decreased with plant age (Figure 5). In contrast, metabolites involved in the Calvin Benson  
246 Cycle were significantly affected by plant age, but only GAP/DHAP and E4P were significantly  
247 different between parts of the canopy, both having larger pools in the subtending leaf  
248 (Supplemental Figure 1).

249

250 One hypothesis for why plants might use the NADP-ME and PEPCK pathway with similar ratios  
251 in subtending leaves and older leaves is to maintain smaller pools of the five transfer acids,  
252 rather than large pools of malate and pyruvate needed for the NADP-ME pathway alone.  
253 Pyruvate, PEP, and aspartate all had strong age effects, decreasing with leaf age, while alanine  
254 increased in the top leaf with plant age, and the malate pool size did not change with plant age.  
255 Because the malate pool is mostly inactive (discussed below), its pool was excluded from a total  
256 transfer acid pool comparison. This combined pool was slightly larger in the top leaf and smaller  
257 in the bottom leaf (p=0.055, ANOVA type II), and decreased with leaf age (p=1.56e-5, ANOVA  
258 type II)

259

### 260 <sup>13</sup>CO<sub>2</sub> labeling in C<sub>3</sub> and C<sub>4</sub> metabolites



261 Differences in pool sizes for each growth stage may be the consequence of cumulative changes  
262 in metabolism over the life of the plant; however, isotopic labeling provides a snapshot of active  
263 metabolism.  $^{13}\text{CO}_2$  was provided to the leaf of 15-day or 55-day old plants, and metabolites  
264 were measured for label incorporation and absolute pool size. These two ages were chosen to  
265 represent plants at the beginning of the vegetative and reproductive growth stages, as well as  
266 contrasting  $\text{C}_4$  metabolite pool sizes. Plants were labeled for up to 5 minutes, and the average  
267 label incorporation in  $\text{C}_4$  shuttle metabolites and several central carbon metabolism metabolites  
268 were quantified (Figure 6A, Supplemental Figure 1). Leaves from 15-day old plants incorporated  
269  $^{13}\text{C}$  label faster than the 55-day old plants, reaching an average labeling amount of 47-55% for  
270 measured Calvin Benson Cycle intermediates (i.e. phosphoglyceric acid (PGA), fructose  
271 biphosphate (FBP), glyceraldehyde 3-phosphate (GAP) and dihydroxyacetone phosphate  
272 (DHAP)) at 15 days compared to 12-27% for 55-day old plants in the top or subtending leaf, in  
273 agreement with the net  $\text{CO}_2$  assimilation data (Figure 1). The  $\text{C}_4$  intermediates were less  
274 enriched at both ages: 15-day old plants contained pyruvate that was 20% average labeled,  
275 24.6% labeled phosphoenolpyruvate (PEP), 35% labeled aspartate, and 8.5% labeled malate.  
276 In the 55-day old plants,  $\text{C}_4$  intermediates were approximately half the average label of the 15-  
277 day old plants after 5 minutes of exposure to  $^{13}\text{CO}_2$  (Supplemental Figure 1).

278  
279 Malate and aspartate predominantly incorporate label from  $^{13}\text{CO}_2$  in the C-4 position, which is  
280 subsequently decarboxylated in the bundle sheath causing loss of the label (Chapman and  
281 Hatch, 1981). Label incorporation in the C1-C3 positions of malate and aspartate comes from  
282 downstream PEP and pyruvate labeling as a result of Calvin Benson Cycle activity. The malate  
283 pool also accumulates little  $^{13}\text{C}$  label due to a large proportion of the malate pool not  
284 participating in photosynthetic metabolism, resulting in a large proportion considered an inactive  
285 pool during stable isotope labeling (Szecowka et al., 2013; Ma et al., 2014; Allen, 2016; Arrivault  
286 et al., 2017). The inactive pool in the 15-day and 55-day plants were similar, with approximately  
287 80% of malate unlabeled after 5 minutes (Figure 6B) and only 10% average labeling  
288 (Supplemental Figure 1), though the final asymptotic value where  $M_0$  levels off is incompletely  
289 defined at the five min time point (Arrivault et al., 2017; AuBuchon-Elder et al., 2020). Looking  
290 more deeply at the distribution of isotopologues, malate and aspartate labeling matched  
291 expectations based on the  $\text{C}_4$  pathways (Figure 6B). The m+1 isotopologue for aspartate  
292 increased rapidly from 0 to 60 seconds to account for 50% of all aspartate in 15-day old plants  
293 and 20-30% in subtending and top leaves of 55-day old plants. Malate m+1 isotopologues

294 accounted for 5-10% of all malate. Very little (<5%) label accumulated in the C1-C3 positions of  
295 malate and aspartate during the first minute of labeling, also consistent with C<sub>4</sub> topology.

296

297 The metabolism of the NADP-ME and PEPCK pathways was calculated in a cross-comparable  
298 way in the three leaves (15-day top, 55-day top, 55-day subtending) using the method described  
299 in Arrivault et al (Arrivault et al., 2017) to calculate n-atom equivalents in the C-4 position of  
300 malate and aspartate. N-atom equivalent measurements for malate and aspartate use the  
301 number of labeled carbons, the metabolite concentration, and the assumption that all malate or  
302 aspartate molecules with at least one <sup>13</sup>C contain label in the C-4 position to quantify labeling  
303 from a molar basis (see Supplemental Table 1). From this calculation, malate and aspartate  
304 labeling were directly compared. During the first 60 seconds of labeling, the C-4 position of  
305 malate labeled at twice the rate of aspartate in the 15-day old plants and 4.3 and 2.6 times  
306 faster in the 55-day old top leaf and subtending leaf, respectively (Figure 6B), reflecting 66.5%  
307 of C<sub>4</sub> activity going through the NADP-ME pathway and 33.5% through PEPCK and indicating a  
308 larger role for aspartate than previously identified, where aspartate only accounted for 10-25%  
309 of the activity of the C<sub>4</sub> shuttle (Chapman and Hatch, 1981; Weissmann et al., 2016; Arrivault et  
310 al., 2017). In the 55-day old plants, the rate of labeling in the C-4 position of malate in the  
311 subtending leaf was approximately one-half the top leaf, while aspartate labeling was consistent  
312 throughout the canopy, resulting in 18.8% of C<sub>4</sub> activity through PEPCK in the top leaf, and  
313 27.9% in the subtending leaf (Figure 6C).

314

#### 315 *Asparagine concentrations in the plant*

316 Asparagine is an important storage and transport form of nitrogen in maize plants (Lohaus et al.,  
317 1998; Lea and Azevedo, 2007) and has been shown to specifically induce PEPCK activity in  
318 grape seeds (Walker et al., 1999). Asparagine can be synthesized from aspartate via  
319 asparagine synthetase and converted back to aspartate through L-asparaginase; however, the  
320 relationship between the C<sub>4</sub> PEPCK and asparagine concentration is not known.

321

322 Asparagine concentration was measured using LC-MS/MS. The asparagine concentration in the  
323 leaf varied from 0.15 μmol mg<sup>-1</sup> to 6.6 μmol mg<sup>-1</sup> and did not have a clear pattern with leaf age  
324 or canopy position in this experiment (Figure 7). Concentrations were more variable than other  
325 metabolites (Supplemental Figure 1), resulting in a decreased ability to observe any trends in  
326 the data. As such, asparagine was very weakly correlated with PEPCK activity (Pearson's R =  
327 0.17) and somewhat correlated with PEPCK expression (Pearson's R = 0.32) in the data.

328 PEPCK activity was more closely correlated with its substrate, aspartate ( $R=0.74$ ), although it  
329 was not correlated with PEPCK expression ( $R=0.07$ ). Aspartate and asparagine correlations  
330 were not correlated ( $R = 0.01$ ). No correlation was observed between asparagine concentration  
331 and PEPCK expression or activity, predominantly because asparagine concentrations were  
332 highly variable within samples, but similar in all plant ages and both canopy positions. To fully  
333 elucidate this relationship in maize leaves, a more targeted approach would be necessary,  
334 focusing on asparagine concentrations in bundle sheath cells. Moreover, asparagine  
335 concentration fluctuates diurnally, with its highest concentrations at night (Harmer et al., 2018;  
336 Kambhampati et al., 2018), so the relationship between asparagine concentration and PEPCK  
337 activity in the leaf may also have a diurnal component which was not assessed in these  
338 experiments.

### 339 **Discussion**

340 The activities of  $C_4$  subtype pathways vary during maize growth; with the greatest difference  
341 between leaves at the top and middle of the canopy, rather than with plant age. PEPCK activity  
342 was consistent between the top leaf and subtending leaf; however, NADP-ME activity  
343 decreased in the older subtending leaf compared to the top leaf, leading to a decreased overall  
344 rate of decarboxylation and changing the ratio of the decarboxylases between the two canopy  
345 positions. Similarly, the PEPCK pathway metabolite aspartate labeled at the same rate in the  
346 top and subtending leaf of 55-day old plants and correlated with PEPCK activity, while malate  
347 labeling decreased by three-fold in the subtending leaf compared to the top leaf. Decreased  
348 malate labeling in the subtending leaf was surprising considering the subtending leaves from all  
349 plant growth stages had larger malate pools than top leaves. These results indicate a large,  
350 inactive pool of malate in the subtending leaf, in addition to the photosynthetically active pool of  
351 malate in plant leaves (Szecowka et al., 2013; Ma et al., 2014; Weissmann et al., 2016; Arrivault  
352 et al., 2017). The large malate pool may serve to buffer the fluctuating light environment within  
353 the canopy or could function as a carbon reserve for remobilization to the grain.

354 Fluctuating environmental conditions, in particular with regard to light, are hypothesized to be a  
355 reason that plants might use a combination of  $C_4$  pathways in parallel (Furbank, 2011; Bellasio  
356 and Griffiths, 2014a; Stitt and Zhu, 2014; Wang et al., 2014). The more stable, typically  
357 unshaded light environment at the top of the canopy may not require the same degree of  
358 metabolic flexibility afforded by parallel pathways and benefits from the efficiency of the NADP-  
359 ME pathway with  $CO_2$  decarboxylation directly in the chloroplast (Wang et al., 2014). The  
360 subtending leaves receive less light in a closed canopy but can have high intensity sun flecks

361 under field conditions and thus may benefit through shared C<sub>4</sub> pathway operation (Bellasio and  
362 Griffiths, 2014a; Stitt and Zhu, 2014; Wang et al., 2014). Our experiments suggest the balanced  
363 activities occur though a reduction in NADP-ME activity and decreased total C<sub>4</sub> shuttling in lower  
364 parts of the canopy (Figure 4, Figure 6), which did not result in a lower carbon assimilation rate  
365 or reduced Calvin Benson Cycle metabolite labeling. Carbon assimilation rates were however  
366 significantly affected by the age of the plant (Figure 2, Supplemental Figure 1). Subtending  
367 leaves maintained the same level of CBC metabolism as leaves at the top of the canopy, likely  
368 as a result of even light distribution through the canopy due to growth in a greenhouse rather  
369 than a dense field canopy (Collison et al., 2020).

370 This study was designed to address differences in C<sub>4</sub> metabolism based on leaf age and canopy  
371 position, such that the same two leaves were compared between plants of different ages. There  
372 were few differences in C<sub>4</sub> metabolism between plants of different ages (i.e. top leaf on plants),  
373 but significant differences in C<sub>4</sub> pathways between leaves in different positions on the same  
374 plant (i.e. microenvironment). These results bring up important possibilities of regulation by light  
375 that differ between leaves on the same plant. Light may play a crucial role in regulating the C<sub>4</sub>  
376 decarboxylases between canopy positions. The relationship between light and C<sub>4</sub> pathway  
377 activity has been studied in the context of different species with different C<sub>4</sub> subtypes (Ubierna  
378 et al., 2013; Sonawane et al., 2018). Less consideration has been given to the plasticity of the  
379 C<sub>4</sub> pathways within a species. NADP-ME is strongly light regulated by light quality (Casati et al.,  
380 1998) and quantity (Hatch and Kagawa, 1976; Bellasio and Griffiths, 2014b), and by time of day,  
381 through phosphorylation, with its activity peaking at two hours after dawn and decreasing slowly  
382 throughout the day (Bovdilova et al., 2019). Leaves positioned lower in the canopy may not  
383 receive the quality and quantity of light to activate NADP-ME to the levels observed at the top of  
384 the canopy (Figure 4, Figure 6). In contrast, PEPCK activity may be unresponsive to light  
385 (Wingler et al., 1999) or potentially negatively regulated by light (Chao et al., 2014); though it  
386 should be noted that the experiments reported here were performed in the greenhouse where  
387 plant leaves are not shaded to the extent they would be in the field. PEPCK expression levels  
388 are more clearly responsive to other environmental conditions such as N supply which could  
389 have effects in leaves subtending the ear (Delgado-Alvarado et al., 2007; Penfield et al., 2012).  
390 N distribution in the canopy also regulates the level of photosynthesis in herbaceous canopies  
391 (Niinemets, 2016).

392 **Conclusions**

393 The top and middle of the canopy and different ages of the plant experience changes in  $C_3$  and  
394  $C_4$  cycle metabolism. Variation in the relative proportion of the two  $C_4$  pathways was strongest  
395 between leaves at the top and bottom of the canopy, while differences in overall photosynthetic  
396 rate were predominantly caused by the age of the plant.  $C_4$  characteristics changed as the leaf  
397 aged, although they did not shift relative to each other, instead generally decreasing overall to  
398 coordinate with decreased  $C_3$  metabolism. At the top of the canopy, the plant predominantly  
399 uses NADP-ME and shifts to more equal use of the two  $C_4$  pathways lower in the canopy, as the  
400 microenvironment in the lower canopy is more variable and the leaves shift to supporting growth  
401 of sink tissues throughout the plant. Plasticity within the plant life cycle and within the canopy is  
402 a potential advantage of the parallel  $C_4$  pathways, allowing fine-tuning of the  $C_4$  pathways to  
403 optimize for specific growth conditions of the leaf.

## 404 **Methods**

### 405 *Plant Growth*

406 Plants were grown in the greenhouse in Saint Louis, MO from February to July 2019. Four  
407 maize plants (genotype W22) were planted at ten day intervals for 90 days. Plants were self-  
408 pollinated upon flowering. Plants were grown in Berger 35, 7% bark medium in 2.5 gallon pots.  
409 Plants were grown with 14-hour day length, 10 hour nights using supplemental light to extend  
410 the day length and when available sunlight was below  $600 \mu\text{mol m}^{-2} \text{s}^{-1}$ . Plant growth  
411 temperature was  $28^{\circ}\text{C}$  day,  $22^{\circ}\text{C}$  night and a minimum 40% relative humidity.

412  
413 Plants were sampled at 100 days after initiation of the experiment. Plants were 10, 20, 30, 40,  
414 50, 60, 70, 80, or 90 days old at the time of sampling. Leaf tissue was collected from the  
415 topmost leaf and the leaf subtending the ear (leaf 13 in W22), when available. For the two oldest  
416 sets of plants (80 or 90 days after sowing), the topmost leaf on each plant was fully senesced  
417 and not sampled. For the three youngest sets of plants (10, 20, or 30 days after sowing), the  
418 subtending leaf had not emerged from the whorl and was not sampled. All measurements were  
419 taken from 10cm leaf segments beginning 20cm from the tip of the leaf.

420

### 421 *Gas Exchange Measurements*

422 Net  $\text{CO}_2$  assimilation was measured using gas exchange measurements on a LI-6800  
423 Photosynthesis System (Li-Cor Inc., Lincoln, Nebraska). Net  $\text{CO}_2$  assimilation was measured at  
424 steady state at 400ppm  $\text{CO}_2$  and 350 followed by  $1500 \mu\text{mol m}^{-2} \text{s}^{-1}$  light. The leaf was clamped  
425 into the instrument head using a 6cm aperture, temperature was controlled at  $25^{\circ}\text{C}$ , and the gas  
426 flow rate was  $500 \mu\text{mol s}^{-1}$ .

427

### 428 *Gene Expression of PEPCK and NADP-ME*

429 Leaf tissue was sampled from a 10cm segment starting 20cm from the leaf tip, from either the  
430 leaf at the top of the canopy or from leaf number 13, which is the leaf below the ear in W22  
431 (subtending leaf). RNA was extracted from 50mg of leaf tissue using Trizol following the  
432 manufacturer instructions (Invitrogen 15596026). Residual genomic DNA was removed using  
433 DNaseI (Invitrogen TURBO DNA-free, AM1907), and first strand cDNA synthesis was  
434 performed using Invitrogen Superscript II (18064022). Gene expression for PEPCK1  
435 (Zm00004b001002) and NADP-ME3 (Zm00004b015828) were quantified via qRT-PCR using a  
436 Roche Light Cycler 480 II using Roche SYBR green I (Roche 04707516001). The delta cT  
437 method was used to quantify relative gene expression of PEPCK1 and NADP-ME3 over time.

438 NAC26 (Zm00004b022707) was used as a housekeeping gene using published primers  
439 (CCGCCGTCAACAGGGAAATCTG, GTAGCACGCCCAAGACCAACAG; (Lin et al.,  
440 2014)Genome-wide identification of housekeeping genes in maize). Primers for PEPCK1 were  
441 forward: CCCGATCAACACCTGGACG and reverse: GACGCACCCATGACAATACC; primers  
442 for NADP-ME3 were forward: GAGTCAGGGCCGTTCAATCT and reverse:  
443 ACAGAGTACCATCCGCGTTG.

444

#### 445 *Enzyme Activity*

446 PEPCK activity was measured using the method of Walker et al (Walker et al., 1999) detailed  
447 on protocols.org (Osorio et al., 2014). Briefly, crude protein was extracted from ~100mg of fresh  
448 leaf tissue in a buffer containing 0.5M bicine-KOH (pH 9.0), 0.2M KCl, 3mM EDTA, 5% (w/v)  
449 PEG-4000, 25mM DTT and 0.4% bovine serum albumin. The extract was centrifuged for 20  
450 minutes and the supernatant was added to a buffer containing 0.5M bicine-KOH (pH 9.0), 3mM  
451 EDTA, 55% w/v) PEG-4000, and 25mM DTT. The sample was incubated for 10 minutes on ice,  
452 centrifuged at 13,000 x g at 4°C for 20 minutes. The supernatant was discarded and the pellet  
453 was resuspended in 10mM bicine-KOH (pH 9.0) with 25mM DTT. Activity was measured in the  
454 carboxylation direction by coupling the reaction with malate dehydrogenase and following the  
455 oxidation of NADH at 340nm using Molecular Devices SpectraMax M2 spectrophotometer. Total  
456 protein was measured using the protein extract for PEPCK activity using Bradford reagent  
457 (Millipore Sigma; Cat: B6916) and commercial bovine serum albumin standards (Thermo Fisher  
458 23208). NADP-malic enzyme activity was measured using the method described in Osorio et al  
459 (Osorio et al., 2014) from Detarsio et al (Detarsio et al., 2003), using 50mg of fresh leaf tissue.  
460 Enzyme activity was measured by following the reduction of NADP<sup>+</sup> at 340nm for 5 minutes.

461

#### 462 *Compositional Analysis*

463 Chlorophyll content was measured using the method of Arnon et al (Arnon, 1949). Amino acid,  
464 sugar and sugar phosphate content was measured using the method described in Czajka et al,  
465 (Czajka et al., 2020). Briefly, metabolites were extracted from 100mg fresh weight of ground leaf  
466 tissue using 3:7 (v/v) methanol:chloroform solution incubated for two hours on a rotator at 4°C.  
467 After two hours, 0.5 mL of ddH<sub>2</sub>O was added, the solution was centrifuged and the supernatant  
468 (aqueous phase) was centrifuged in 3KDa filters, frozen, lyophilized, and resuspended in 50uL  
469 1:1 methanol:ddH<sub>2</sub>O. Metabolite quantities were measured using LC-MS using a Shimadzu  
470 Prominence-xR UFLC system and a SCIEX hybrid triple quadrupole-linear ion trap MS  
471 equipped with Turbo V<sup>TM</sup> electrospray ionization source for separation and detection of

472 metabolites, and samples were injected into an InfinityLab Poroshell 120 HILIC-Z (2.1 x 100  
473 mm, 2.7  $\mu$ m, Agilent Technologies) column.

474

#### 475 *Stable isotope labeling using $^{13}\text{CO}_2$*

476 Isotopic labeling was performed on plants from two of the stages, 15 days and 55 days after  
477 sowing. For 15-day old plants, the top collared leaf was sampled, and for 55-day old plants, both  
478 the top collared leaf and the subtending leaf were used. The 15-day old plants were selected to  
479 represent the growth stage commonly characterized for  $\text{C}_4$  pathway labeling (Chapman and  
480 Hatch, 1981; Weissmann et al., 2016; Arrivault et al., 2017), where young maize leaves use the  
481 NADP-ME pathway for 75-90% of metabolism, relying on the PEPCK pathway as a minor  
482 contributor. The 55-day sample was selected to represent plants that have generated all of their  
483 leaves, reached the end of vegetative growth, and are approaching the developmental shift at  
484 anthesis. Labeling in central carbon metabolites was measured using  $^{13}\text{CO}_2$  provided to the leaf  
485 with a hand-held clamp for 0, 20, 60, or 300 seconds to generate a time course of label  
486 incorporation. Leaves were freeze clamped at the end of each time interval, flash frozen in liquid  
487 nitrogen, and stored at  $-80^\circ\text{C}$  until further processing. Metabolites were extracted in  
488 chloroform:methanol as above, and metabolite labeling and pool size were measured by LC-  
489 MS/MS on a Qtrap6500 (Chu et al, in prep; (Czajka et al., 2020)). Samples were corrected for  
490 natural abundance of  $^{13}\text{C}$  using IsoCorrectoR (Heinrich et al., 2018).

491

#### 492 *Statistical Analysis*

493 ANOVA comparisons were performed using two-way ANOVAs with factors canopy position  
494 (leaf) and plant age, with the Anova function in the car package in R (Fox and Weisberg, 2018)  
495 to use a type II ANOVA to be able to compare factors with unequal sample sizes.

496

#### 497 **Acknowledgements**

498 The authors would like to thank the Donald Danforth Plant Science Center Plant Growth Facility  
499 and Donald Danforth Plant Science Center Proteomics and Mass Spectrometry Facility. Thank  
500 you to Emma Smith, Emily Frankenreiter, and Genesis Hudson for assistance with performing  
501 tissue sampling.



## 502 **Figures**

503 **Figure 1: Experimental Design:** Plants were grown at ten day intervals in the greenhouse to  
504 generate a gradient of maize development which could be sampled on the same day. Nine  
505 individual time points were used and captured maize development from the V3 stage until  
506 physiological maturity. The leaf at the top of the canopy for each time point was sampled until  
507 the top leaf senesced at 90 days after sowing. Also sampled was leaf 13, which subtends the  
508 ear in genotype W22. Leaf 13 emerged from the whorl at 50 days after sowing.

509  
510 **Figure 2: Measures of overall photosynthesis:** A.) Net CO<sub>2</sub> assimilation (A) was measured at  
511 two light levels using a LI-COR 6800 gas exchange instrument. B.) Total chlorophyll was  
512 measured using a spectrometric assay. C.) Chlorophyll a to b ratio. All data are means ± sd of  
513 3-4 replicate plants.

514  
515 **Figure 3: Gene expression differences:** A.) Expression of NADP-ME3 (Zm00004b015828) and  
516 PEPCK1 (Zm00004b001002) in the maize gene expression atlas (Stelpflug et al, 2016)  
517 decreased with plant age, and the ratio of NADP-ME3 (gray) to PEPCK1 (blue) decreased in  
518 older plants. B.) Relative gene expression for PEPCK1 and NADP-ME3 was quantified using  
519 qPCR. Data are means ± sd of 3-4 replicate plants.

520  
521 **Figure 4: Enzyme activity assays:** *In vitro* activities of NADP-ME (gray) and PEPCK (blue)  
522 from whole leaf segments of maize leaves at nine growth stages from the top or subtending leaf.  
523 Data are means ± sd of 3-4 replicate plants.

524  
525 **Figure 5: C<sub>4</sub> transfer acid quantification:** Malate and aspartate pools were quantified using an  
526 LC-MS approach and normalized by sample fresh weight. Malate pools (black) were larger than  
527 aspartate pools (blue) for all measured time points. Data are means ± sd of 3-4 replicate plants.

528  
529 **Figure 6: C<sub>4</sub> transfer acid labeling:** A.) Quantitation of malate and aspartate pools using LC-  
530 MS. Malate (gray); aspartate (blue). B.) Time course of labeling for malate and aspartate. Mass  
531 isotopologs (m<sub>n</sub>) represent malate or aspartate molecules that have incorporated n molecules of  
532 <sup>13</sup>C. C.) Moles of <sup>13</sup>C in the C-4 position of malate (gray) and aspartate (blue) using the method  
533 of (Arrivault et al., 2017).

534  
535 **Figure 7: Asparagine:** asparagine concentration during plant growth measured by LC-MS  
536 normalized by sample fresh weight. Data are means ± sd of 3-4 replicate plants.

537

538

## 539 **Supplemental Data**

540

541 **Supplemental Table 1:** Calculations to determine degree of labeling in the C-4 position of malate  
542 and aspartate.

543

544 **Supplemental Figure 1:** A.) Metabolite quantitation of C<sub>4</sub> intermediates. PEP:  
545 phospho*eno*/pyruvate. B.) Metabolite quantitation of Calvin Benson Cycle intermediates which  
546 were able to be quantified. TP: Triose phosphate (i.e. GAP and DHAP: Glyceraldehyde 3-  
547 phosphate and Dihydroxyacetone phosphate), FBP: Fructose 1,6-bisphosphate; E4P: Erythrose  
548 4-phosphate; S7P: Sedoheptulose 7-phosphate; R5P: Ribose 5-phosphate.

549

550 **Supplemental Figure 2:** Average labeling in C<sub>3</sub> and C<sub>4</sub> metabolites during the five minute time  
551 course. PEP: phospho*eno*/pyruvate, PGA: phosphoglyceric acid, FBP: fructose 1,6-  
552 bisphosphate, TP: triose phosphate (i.e. GAP and DHAP: glyceraldehyde 3-phosphate and

553 dihydroxyacetone phosphate), UDPG: uridine diphosphate glucose, 2OG: 2-oxoglutarate, ASN:  
554 asparagine, GLN: glutamine, Glu: glutamate.

555

556 Supplemental Figure 3: Isotopologue distribution graphs for labeled metabolites during the five  
557 minute time course. PEP: phospho*eno*pyruvate, PGA: phosphoglyceric acid, FBP: fructose 1,6-  
558 biphosphate, TP: triose phosphate (i.e. GAP and DHAP: glyceraldehyde 3-phosphate and  
559 dihydroxyacetone phosphate), UDPG: uridine diphosphate glucose, 2OG: 2-oxoglutarate, ASN:  
560 asparagine, GLN: glutamine, Glu: glutamate.

561 **References**

- 562 Allen DK (2016) Quantifying plant phenotypes with isotopic labeling & metabolic flux analysis.  
563 *Curr Opin Biotechnol* 37: 45–52
- 564 Arnon DI (1949) COPPER ENZYMES IN ISOLATED CHLOROPLASTS.  
565 POLYPHENOLOXIDASE IN BETA VULGARIS. *Plant Physiol* 24: 1–15
- 566 Arrivault S, Obata T, Szecówka M, Mengin V, Guenther M, Hoehne M, Fernie AR, Stitt M (2017)  
567 Metabolite pools and carbon flow during C4 photosynthesis in maize: <sup>13</sup>CO<sub>2</sub> labeling  
568 kinetics and cell type fractionation. *J Exp Bot* 68: 283–298
- 569 AuBuchon-Elder T, Coneva V, Goad DM, Jenkins LM, Yu Y, Allen DK, Kellogg EA (2020) Sterile  
570 Spikelets Contribute to Yield in Sorghum and Related Grasses. *Plant Cell* 32: 3500–3518
- 571 Bahrami AR, Chen ZH, Walker RP, Leegood RC, Gray JE (2001) Ripening-related occurrence  
572 of phosphoenolpyruvate carboxykinase in tomato fruit. *Plant Mol Biol* 47: 499–506
- 573 Baker NR, Long SP, Ort DR (1988) Photosynthesis and temperature, with particular reference  
574 to effects on quantum yield. *Symp Soc Exp Biol* 42: 347–375
- 575 Bellasio C, Griffiths H (2014a) The Operation of Two Decarboxylases, Transamination, and  
576 Partitioning of C4 Metabolic Processes between Mesophyll and Bundle Sheath Cells Allows  
577 Light Capture To Be Balanced for the Maize C4 Pathway. *Plant Physiol* 164: 466–480
- 578 Bellasio C, Griffiths H (2014b) Acclimation of C4 metabolism to low light in mature maize leaves  
579 could limit energetic losses during progressive shading in a crop canopy. *J Exp Bot* 65:  
580 3725–3736
- 581 Björkman O (1981) Responses to different quantum flux densities. *Physiological plant ecology I*
- 582 Boardman NK (1977) Comparative Photosynthesis of Sun and Shade Plants. *Annu Rev Plant*  
583 *Physiol* 28: 355–377
- 584 Bovdilova A, Alexandre BM, Höppner A, Luís IM, Alvarez CE, Bickel D, Gohlke H, Decker C,  
585 Nagel-Steger L, Alseekh S, et al (2019) Posttranslational Modification of the NADP-Malic  
586 Enzyme Involved in C4 Photosynthesis Modulates the Enzymatic Activity during the Day.  
587 *Plant Cell* 31: 2525–2539
- 588 Cañas RA, Quilleré I, Lea PJ, Hirel B (2010) Analysis of amino acid metabolism in the ear of  
589 maize mutants deficient in two cytosolic glutamine synthetase isoenzymes highlights the  
590 importance of asparagine for nitrogen translocation within sink organs. *Plant Biotechnol J* 8:  
591 966–978
- 592 Casati P, Drincovich MF, Andreo CS, Donahue R, Edwards GE (1998) UV-B, red and far-red  
593 light regulate induction of the C4 isoform of NADP-malic enzyme in etiolated maize  
594 seedlings. *Funct Plant Biol* 25: 701–708
- 595 Chao Q, Liu X-Y, Mei Y-C, Gao Z-F, Chen Y-B, Qian C-R, Hao Y-B, Wang B-C (2014) Light-  
596 regulated phosphorylation of maize phosphoenolpyruvate carboxykinase plays a vital role  
597 in its activity. *Plant Mol Biol* 85: 95–105
- 598 Chapman KSR, Hatch MD (1981) Aspartate Decarboxylation in Bundle Sheath Cells of Zea

- 599 mays and Its Possible Contribution to C3 Photosynthesis. *Funct Plant Biol* 8: 237–248
- 600 Chen Y, Wu D, Mu X, Xiao C, Chen F, Yuan L, Mi G (2016) Vertical Distribution of  
601 Photosynthetic Nitrogen Use Efficiency and Its Response to Nitrogen in Field-Grown Maize.  
602 *Crop Sci* 56: 397–407
- 603 Collison RF, Raven EC, Pignon CP, Long SP (2020) Light, Not Age, Underlies the  
604 Maladaptation of Maize and *Miscanthus* Photosynthesis to Self-Shading. *Front Plant Sci*  
605 11: 783
- 606 Czajka JJ, Kambhampati S, Tang YJ, Wang Y, Allen DK (2020) Application of Stable Isotope  
607 Tracing to Elucidate Metabolic Dynamics During *Yarrowia lipolytica*  $\alpha$ -Ionone Fermentation.  
608 *iScience* 23: 100854
- 609 Delgado-Alvarado A, Walker RP, Leegood RC (2007) Phosphoenolpyruvate carboxykinase in  
610 developing pea seeds is associated with tissues involved in solute transport and is  
611 nitrogen-responsive. *Plant Cell Environ* 30: 225–235
- 612 Detarsio E, Wheeler MCG, Bermúdez VAC, Andreo CS, Drincovich MF (2003) Maize C4 NADP-  
613 malic enzyme: Expression in *Escherichia coli* and characterization of site-directed mutants  
614 at the putative nucleotide-binding sites. *J Biol Chem* 278: 13757–13764
- 615 Dwyer LM, Stewart DW (1986) Effect of leaf age and position on net photosynthetic rates in  
616 maize (*Zea mays* L.). *Agric For Meteorol* 37: 29–46
- 617 Evans JR, Poorter H (2001) Photosynthetic acclimation of plants to growth irradiance: the  
618 relative importance of specific leaf area and nitrogen partitioning in maximizing carbon gain.  
619 *Plant Cell Environ* 24: 755–767
- 620 Fox J, Weisberg S (2018) *An R Companion to Applied Regression*. SAGE Publications
- 621 Furbank RT (2011) Evolution of the C(4) photosynthetic mechanism: are there really three C(4)  
622 acid decarboxylation types? *J Exp Bot* 62: 3103–3108
- 623 Ghannoum O, Evans JR, Chow WS, Andrews TJ, Conroy JP, von Caemmerer S (2005) Faster  
624 Rubisco is the key to superior nitrogen-use efficiency in NADP-malic enzyme relative to  
625 NAD-malic enzyme C4 grasses. *Plant Physiol* 137: 638–650
- 626 Harmer SL, Covington MF, Bläsing O, Stitt M (2018) Circadian regulation of global gene  
627 expression and metabolism. *Annual Plant Reviews online* 133–165
- 628 Hatch MD, Kagawa T (1976) Photosynthetic activities of isolated bundle sheath cells in relation  
629 to differing mechanisms of C-4 pathway photosynthesis. *Arch Biochem Biophys* 175: 39–53
- 630 Heinrich P, Kohler C, Ellmann L, Kuerner P, Spang R, Oefner PJ, Dettmer K (2018) Correcting  
631 for natural isotope abundance and tracer impurity in MS-, MS/MS- and high-resolution-  
632 multiple-tracer-data from stable isotope labeling experiments with IsoCorrectoR. *Sci Rep* 8:  
633 17910
- 634 Hernández-Sebastià C, Marsolais F, Saravitz C, Israel D, Dewey RE, Huber SC (2005) Free  
635 amino acid profiles suggest a possible role for asparagine in the control of storage-product  
636 accumulation in developing seeds of low-and high-protein soybean lines. *J Exp Bot* 56:  
637 1951–1963

- 638 Hikosaka K, Terashima I (1995) A model of the acclimation of photosynthesis in the leaves of  
639 C3 plants to sun and shade with respect to nitrogen use. *Plant Cell Environ* 18: 605–618
- 640 Kambhampati S, Ajewole E, Marsolais F (2018) Advances in Asparagine Metabolism. *In* FM  
641 Cánovas, U Lüttge, R Matyssek, eds, *Progress in Botany Vol. 79*. Springer International  
642 Publishing, Cham, pp 49–74
- 643 Kanai R, Edwards GE (1999) The biochemistry of C4 photosynthesis. *C4 plant biology* 49: 87
- 644 Khamis S, Lamaze T, Farineau J (1992) Effect of nitrate limitation on the photosynthetically  
645 active pools of aspartate and malate in maize, a NADP malic enzyme C 4 plant. *Physiol*  
646 *Plant* 85: 223–229
- 647 Lea PJ, Azevedo RA (2007) Nitrogen use efficiency. 2. Amino acid metabolism. *Ann Appl Biol*  
648 151: 269–275
- 649 Lin F, Jiang L, Liu Y, Lv Y, Dai H, Zhao H (2014) Genome-wide identification of housekeeping  
650 genes in maize. *Plant Mol Biol* 86: 543–554
- 651 Lohaus G, Büker M, Hußmann M, Soave C, Heldt H-W (1998) Transport of amino acids with  
652 special emphasis on the synthesis and transport of asparagine in the Illinois Low Protein  
653 and Illinois High Protein strains of maize. *Planta* 205: 181–188
- 654 Ma F, Jazmin LJ, Young JD, Allen DK (2014) Isotopically nonstationary <sup>13</sup>C flux analysis of  
655 changes in *Arabidopsis thaliana* leaf metabolism due to high light acclimation. *Proceedings*  
656 *of the National Academy of Sciences* 111: 16967–16972
- 657 Meister M, Agostino A, Hatch MD (1996) The roles of malate and aspartate in C4 photosynthetic  
658 metabolism of *Flaveria bidentis* (L.). *Planta* 199: 262–269
- 659 Niinemets Ü (2016) Leaf age dependent changes in within-canopy variation in leaf functional  
660 traits: a meta-analysis. *J Plant Res* 129: 313–338
- 661 Osorio S, Vallarino JG, Szecowka M, Ufaz S, Tzin V, Angelovici R, Galili G, Fernie AR (2014)  
662 Extraction and Measurement the Activities of Cytosolic Phosphoenolpyruvate  
663 Carboxykinase (PEPCK) and Plastidic NADP-dependent Malic Enzyme (ME) on Tomato  
664 (*Solanum lycopersicum*). *Bio-protocol* 4: e1122–e1122
- 665 Pandurangan S, Pajak A, Molnar SJ, Cober ER, Dhaubhadel S, Hernández-Sebastià C, Kaiser  
666 WM, Nelson RL, Huber SC, Marsolais F (2012) Relationship between asparagine  
667 metabolism and protein concentration in soybean seed. *J Exp Bot* 63: 3173–3184
- 668 Penfield S, Clements S, Bailey KJ, Gilday AD, Leegood RC, Gray JE, Graham IA (2012)  
669 Expression and manipulation of phosphoenolpyruvate carboxykinase 1 identifies a role for  
670 malate metabolism in stomatal closure. *Plant J* 69: 679–688
- 671 Pengelly JJJ, Sirault XRR, Tazoe Y, Evans JR, Furbank RT, von Caemmerer S (2010) Growth  
672 of the C4 dicot *Flaveria bidentis*: photosynthetic acclimation to low light through shifts in leaf  
673 anatomy and biochemistry. *J Exp Bot* 61: 4109–4122
- 674 Pick TR, Bräutigam A, Schlüter U, Denton AK, Colmsee C, Scholz U, Fahnenstich H,  
675 Pieruschka R, Rascher U, Sonnewald U, et al (2011) Systems analysis of a maize leaf  
676 developmental gradient redefines the current C4 model and provides candidates for

- 677 regulation. *Plant Cell* 23: 4208–4220
- 678 Pinto H, Powell JR, Sharwood RE, Tissue DT, Ghannoum O (2016) Variations in nitrogen use  
679 efficiency reflect the biochemical subtype while variations in water use efficiency reflect the  
680 evolutionary lineage of C4 grasses at inter-glacial CO<sub>2</sub>. *Plant Cell Environ* 39: 514–526
- 681 Pinto H, Sharwood RE, Tissue DT, Ghannoum O (2014) Photosynthesis of C<sub>3</sub>, C<sub>3</sub>–C<sub>4</sub>, and C<sub>4</sub>  
682 grasses at glacial CO<sub>2</sub>. *J Exp Bot* 65: 3669–3681
- 683 Pons TL (2016) Regulation of Leaf Traits in Canopy Gradients. *In* K Hikosaka, Ü Niinemets,  
684 NPR Anten, eds, *Canopy Photosynthesis: From Basics to Applications*. Springer  
685 Netherlands, Dordrecht, pp 143–168
- 686 Sage RF, Christin P-A, Edwards EJ (2011) The C(4) plant lineages of planet Earth. *J Exp Bot*  
687 62: 3155–3169
- 688 Seebauer JR, Moose SP, Fabbri BJ, Crossland LD, Below FE (2004) Amino acid metabolism in  
689 maize earshoots. Implications for assimilate preconditioning and nitrogen signaling. *Plant*  
690 *Physiol* 136: 4326–4334
- 691 Sommer M, Bräutigam A, Weber APM (2012) The dicotyledonous NAD malic enzyme C4 plant  
692 *Cleome gynandra* displays age-dependent plasticity of C4 decarboxylation biochemistry.  
693 *Plant Biol* 14: 621–629
- 694 Sonawane BV, Sharwood RE, Whitney S, Ghannoum O (2018) Shade compromises the  
695 photosynthetic efficiency of NADP-ME less than that of PEP-CK and NAD-ME C4 grasses.  
696 *J Exp Bot* 69: 3053–3068
- 697 Stelpflug SC, Sekhon RS, Vaillancourt B, Hirsch CN, Buell CR, de Leon N, Kaeppler SM (2016)  
698 An Expanded Maize Gene Expression Atlas based on RNA Sequencing and its Use to  
699 Explore Root Development. *Plant Genome*. doi: 10.3835/plantgenome2015.04.0025
- 700 Stitt M, Zhu X-G (2014) The large pools of metabolites involved in intercellular metabolite  
701 shuttles in C4 photosynthesis provide enormous flexibility and robustness in a fluctuating  
702 light environment. *Plant Cell Environ* 37: 1985–1988
- 703 Subedi KD, Ma BL (2005) Ear Position, Leaf Area, and Contribution of Individual Leaves to  
704 Grain Yield in Conventional and Leafy Maize Hybrids. *Crop Sci* 45: 2246–2257
- 705 Sugiyama T, Mizuno M, Hayashi M (1984) Partitioning of nitrogen among ribulose-1, 5-  
706 bisphosphate carboxylase/oxygenase, phosphoenolpyruvate carboxylase, and pyruvate  
707 orthophosphate dikinase as related to biomass productivity in maize seedlings. *Plant*  
708 *Physiol* 75: 665–669
- 709 Szecowka M, Heise R, Tohge T, Nunes-Nesi A, Vosloh D, Huege J, Feil R, Lunn J, Nikoloski Z,  
710 Stitt M, et al (2013) Metabolic fluxes in an illuminated *Arabidopsis* rosette. *Plant Cell* 25:  
711 694–714
- 712 Taub DR, Lerdau MT (2000) Relationship between leaf nitrogen and photosynthetic rate for  
713 three NAD-ME and three NADP-ME C4 grasses. *Am J Bot* 87: 412–417
- 714 Tazoe Y, Noguchi K, Terashima I (2006) Effects of growth light and nitrogen nutrition on the  
715 organization of the photosynthetic apparatus in leaves of a C4 plant, *Amaranthus cruentus*.

- 716 Plant Cell Environ 29: 691–700
- 717 Ubierna N, Sun W, Kramer DM, Cousins AB (2013) The efficiency of C4 photosynthesis under  
718 low light conditions in *Zea mays*, *Miscanthus x giganteus* and *Flaveria bidentis*. *Plant Cell*  
719 *Environ* 36: 365–381
- 720 Walker RP, Acheson RM, Técsi LI, Leegood RC (1997) Phosphoenolpyruvate Carboxykinase in  
721 C4 Plants: Its Role and Regulation. *Funct Plant Biol* 24: 459–468
- 722 Walker RP, Chen ZH, Tecsli LI, Famiani F, Lea PJ, Leegood RC (1999) Phosphoenolpyruvate  
723 carboxykinase plays a role in interactions of carbon and nitrogen metabolism during grape  
724 seed development. *Planta* 210: 9–18
- 725 Walters RG (2005) Towards an understanding of photosynthetic acclimation. *J Exp Bot* 56:  
726 435–447
- 727 Wang Y, Bräutigam A, Weber APM, Zhu X-G (2014) Three distinct biochemical subtypes of C4  
728 photosynthesis? A modelling analysis. *J Exp Bot* 65: 3567–3578
- 729 Ward DA, Woolhouse HW (1986) Comparative effects of light during growth on the  
730 photosynthetic properties of NADP-ME type C4 grasses from open and shaded habitats. II.  
731 Photosynthetic enzyme activities and metabolism. *Plant Cell Environ* 9: 271–277
- 732 Weissmann S, Ma F, Furuyama K, Gierse J, Berg H, Shao Y, Taniguchi M, Allen DK, Brutnell  
733 TP (2016) Interactions of C4 Subtype Metabolic Activities and Transport in Maize Are  
734 Revealed through the Characterization of DCT2 Mutants. *Plant Cell* 28: 466–484
- 735 Wingler A, Walker RP, Chen ZH, Leegood RC (1999) Phosphoenolpyruvate carboxykinase is  
736 involved in the decarboxylation of aspartate in the bundle sheath of maize. *Plant Physiol*  
737 120: 539–546

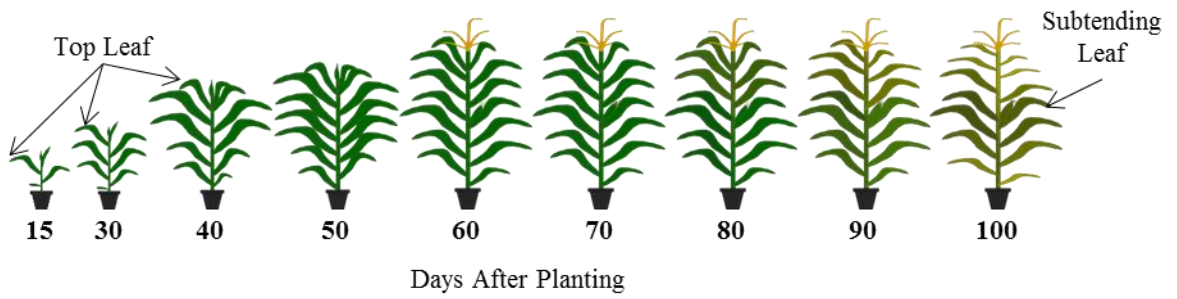
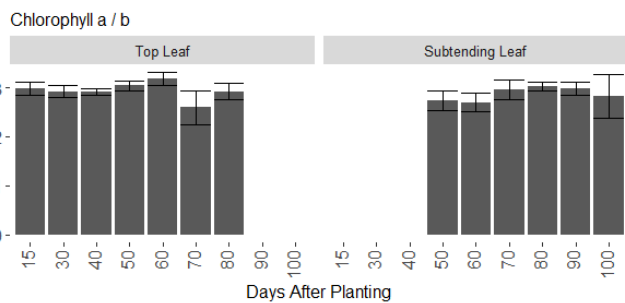
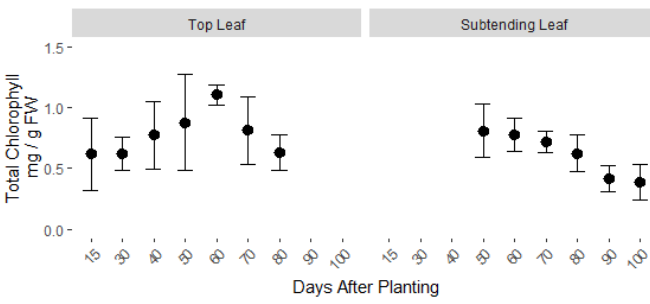
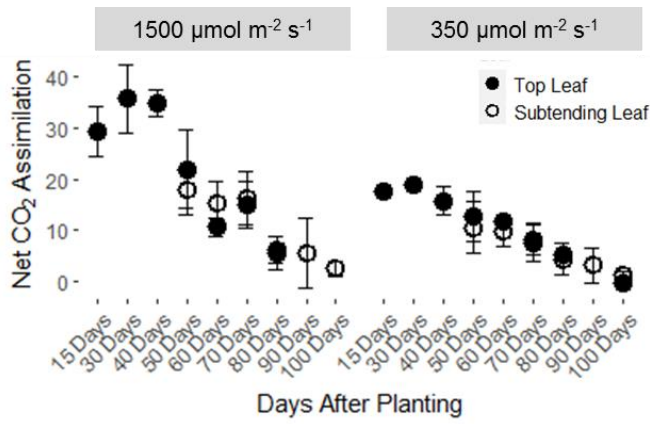
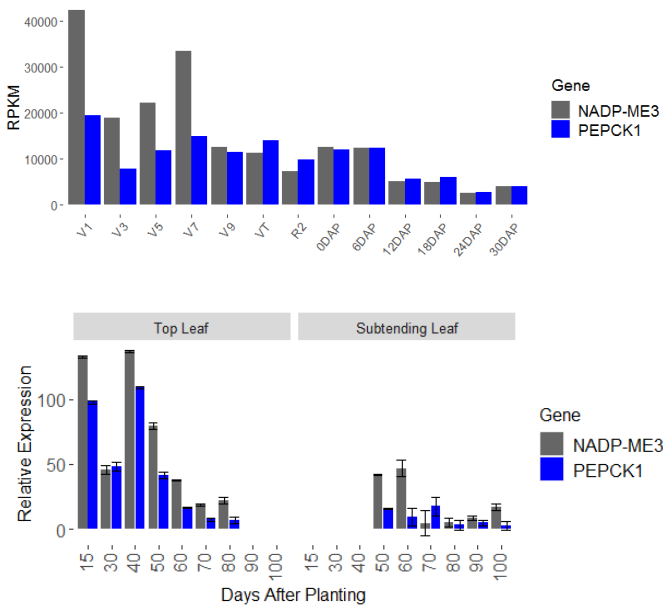


Figure 1: **Experimental Design:** Plants were grown at ten day intervals in the greenhouse to generate a gradient of maize development which could be sampled on the same day. Nine individual time points were used and captured maize development from the V3 stage until physiological maturity. The leaf at the top of the canopy for each time point was sampled until the top leaf senesced at 90 days after sowing. Also sampled was leaf 13, which subtends the ear in genotype W22. Leaf 13 emerged from the whorl at 50 days after sowing.





**Figure 2: Measures of overall photosynthesis:** A.) Net CO<sub>2</sub> assimilation (A) was measured at two light levels using a LI-COR 6800 gas exchange instrument. B.) Total chlorophyll was measured using a spectrometric assay. C.) Chlorophyll a to b ratio. All data are means ± standard deviation of 3-4 replicate plants.



**Figure 3: Gene expression differences: A.)** Expression of NADP-ME3 (Zm00004b015828) and PEPCK1 (Zm00004b001002) in the maize gene expression atlas (Stelpflug et al, 2016) decreased with plant age, and the ratio of NADP-ME3 (gray) to PEPCK1 (blue) decreased in older plants. B.) Relative gene expression for PEPCK1 and NADP-ME3 was quantified using qPCR. Data are means  $\pm$  sd of 3-4 replicate plants.

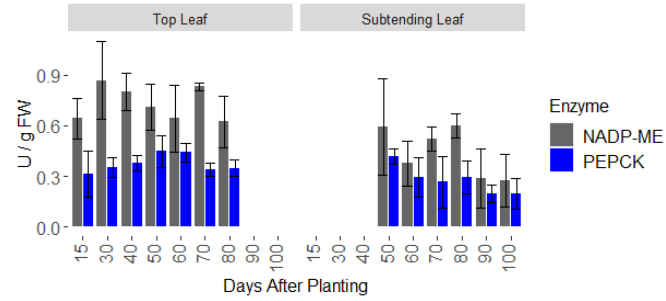


Figure 4: **Enzyme activity assays:** *In vitro* activities of NADP-ME (gray) and PEPCK (blue) from whole leaf segments of maize leaves at nine growth stages from the top or subtending leaf. Data are means  $\pm$  sd of 3-4 replicate plants. U:  $\mu$ mol NADH oxidation (PEPCK) or NADP<sup>+</sup> reduction (NADP-ME) per minute.

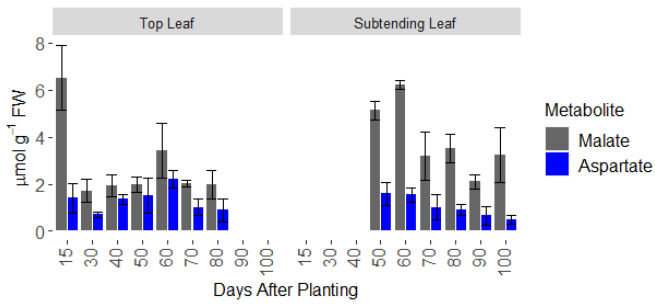


Figure 5: **C<sub>4</sub> transfer acid quantification:** Malate and aspartate pools were quantified using an LC-MS approach and normalized by sample fresh weight. Malate pools (black) were larger than aspartate pools (blue) for all measured time points. Data are means  $\pm$  sd of 3-4 replicate plants.

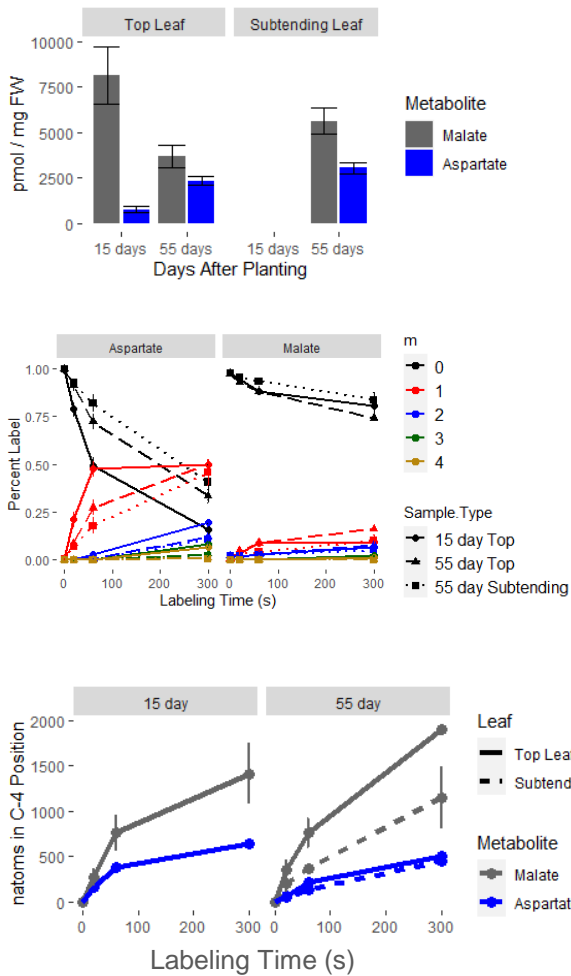


Figure 6: **C<sub>4</sub> transfer acid labeling**: A.) Quantitation of malate and aspartate pools using LC-MS. Malate (gray); aspartate (blue). B.) Time course of labeling for malate and aspartate. Mass isotopologs ( $m_n$ ) represent malate or aspartate molecules that have incorporated  $n$  molecules of  $^{13}\text{C}$ . C.) Moles of  $^{13}\text{C}$  in the C-4 position of malate (gray) and aspartate (blue) using the method of Arrivault et al. (Arrivault et al., 2017).

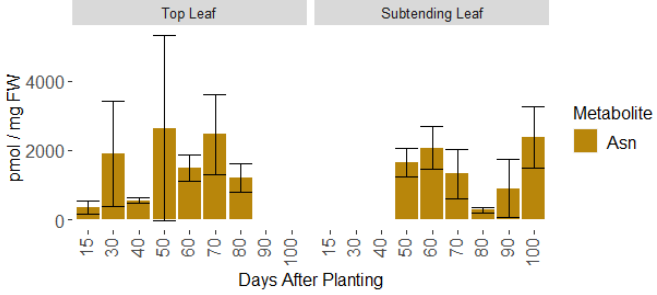


Figure 7: Asparagine concentration during plant growth measured by LC-MS normalized by sample fresh weight. Data are means  $\pm$  sd of 3-4 replicate plants.

## Parsed Citations

- Allen DK (2016)** Quantifying plant phenotypes with isotopic labeling & metabolic flux analysis. *Curr Opin Biotechnol* 37: 45–52  
Google Scholar: [Author Only](#) [Title Only](#) [Author and Title](#)
- Arnon DI (1949)** COPPER ENZYMES IN ISOLATED CHLOROPLASTS. POLYPHENOLOXIDASE IN BETA VULGARIS. *Plant Physiol* 24: 1–15  
Google Scholar: [Author Only](#) [Title Only](#) [Author and Title](#)
- Arrivault S, Obata T, Szczówka M, Mengin V, Guenther M, Hoehne M, Fernie AR, Stitt M (2017)** Metabolite pools and carbon flow during C4 photosynthesis in maize: <sup>13</sup>C<sub>2</sub> labeling kinetics and cell type fractionation. *J Exp Bot* 68: 283–298  
Google Scholar: [Author Only](#) [Title Only](#) [Author and Title](#)
- AuBuchon-Elder T, Coneva V, Goad DM, Jenkins LM, Yu Y, Allen DK, Kellogg EA (2020)** Sterile Spikelets Contribute to Yield in Sorghum and Related Grasses. *Plant Cell* 32: 3500–3518  
Google Scholar: [Author Only](#) [Title Only](#) [Author and Title](#)
- Bahrani AR, Chen ZH, Walker RP, Leegood RC, Gray JE (2001)** Ripening-related occurrence of phosphoenolpyruvate carboxykinase in tomato fruit. *Plant Mol Biol* 47: 499–506  
Google Scholar: [Author Only](#) [Title Only](#) [Author and Title](#)
- Baker NR, Long SP, Ort DR (1988)** Photosynthesis and temperature, with particular reference to effects on quantum yield. *Symp Soc Exp Biol* 42: 347–375  
Google Scholar: [Author Only](#) [Title Only](#) [Author and Title](#)
- Bellasio C, Griffiths H (2014a)** The Operation of Two Decarboxylases, Transamination, and Partitioning of C4 Metabolic Processes between Mesophyll and Bundle Sheath Cells Allows Light Capture To Be Balanced for the Maize C4 Pathway. *Plant Physiol* 164: 466–480  
Google Scholar: [Author Only](#) [Title Only](#) [Author and Title](#)
- Bellasio C, Griffiths H (2014b)** Acclimation of C4 metabolism to low light in mature maize leaves could limit energetic losses during progressive shading in a crop canopy. *J Exp Bot* 65: 3725–3736  
Google Scholar: [Author Only](#) [Title Only](#) [Author and Title](#)
- Björkman O (1981)** Responses to different quantum flux densities. *Physiological plant ecology I*  
Google Scholar: [Author Only](#) [Title Only](#) [Author and Title](#)
- Boardman NK (1977)** Comparative Photosynthesis of Sun and Shade Plants. *Annu Rev Plant Physiol* 28: 355–377  
Google Scholar: [Author Only](#) [Title Only](#) [Author and Title](#)
- Bovdilova A, Alexandre BM, Höppner A, Luís IM, Alvarez CE, Bickel D, Gohlke H, Decker C, Nagel-Steger L, Alosekh S, et al (2019)** Posttranslational Modification of the NADP-Malic Enzyme Involved in C4 Photosynthesis Modulates the Enzymatic Activity during the Day. *Plant Cell* 31: 2525–2539  
Google Scholar: [Author Only](#) [Title Only](#) [Author and Title](#)
- Cañas RA, Quilleré I, Lea PJ, Hirel B (2010)** Analysis of amino acid metabolism in the ear of maize mutants deficient in two cytosolic glutamine synthetase isoenzymes highlights the importance of asparagine for nitrogen translocation within sink organs. *Plant Biotechnol J* 8: 966–978  
Google Scholar: [Author Only](#) [Title Only](#) [Author and Title](#)
- Casati P, Drincovich MF, Andreo CS, Donahue R, Edwards GE (1998)** UV-B, red and far-red light regulate induction of the C4 isoform of NADP-malic enzyme in etiolated maize seedlings. *Funct Plant Biol* 25: 701–708  
Google Scholar: [Author Only](#) [Title Only](#) [Author and Title](#)
- Chao Q, Liu X-Y, Mei Y-C, Gao Z-F, Chen Y-B, Qian C-R, Hao Y-B, Wang B-C (2014)** Light-regulated phosphorylation of maize phosphoenolpyruvate carboxykinase plays a vital role in its activity. *Plant Mol Biol* 85: 95–105  
Google Scholar: [Author Only](#) [Title Only](#) [Author and Title](#)
- Chapman KSR, Hatch MD (1981)** Aspartate Decarboxylation in Bundle Sheath Cells of Zea mays and Its Possible Contribution to C3 Photosynthesis. *Funct Plant Biol* 8: 237–248  
Google Scholar: [Author Only](#) [Title Only](#) [Author and Title](#)
- Chen Y, Wu D, Mu X, Xiao C, Chen F, Yuan L, Mi G (2016)** Vertical Distribution of Photosynthetic Nitrogen Use Efficiency and Its Response to Nitrogen in Field-Grown Maize. *Crop Sci* 56: 397–407  
Google Scholar: [Author Only](#) [Title Only](#) [Author and Title](#)
- Collison RF, Raven EC, Pignon CP, Long SP (2020)** Light, Not Age, Underlies the Maladaptation of Maize and Miscanthus Photosynthesis to Self-Shading. *Front Plant Sci* 11: 783  
Google Scholar: [Author Only](#) [Title Only](#) [Author and Title](#)
- Czajka JJ, Kambhampati S, Tang YJ, Wang Y, Allen DK (2020)** Application of Stable Isotope Tracing to Elucidate Metabolic Dynamics During *Yarrowia lipolytica*  $\alpha$ -Ionone Fermentation. *iScience* 23: 100854  
Google Scholar: [Author Only](#) [Title Only](#) [Author and Title](#)

- Delgado-Alvarado A, Walker RP, Leegood RC (2007) Phosphoenolpyruvate carboxykinase in developing pea seeds is associated with tissues involved in solute transport and is nitrogen-responsive. *Plant Cell Environ* 30: 225–235**  
Google Scholar: [Author Only](#) [Title Only](#) [Author and Title](#)
- Detarsio E, Wheeler MCG, Bermúdez VAC, Andreo CS, Drincovich MF (2003) Maize C4 NADP-malic enzyme: Expression in escherichia coli and characterization of site-directed mutants at the putative nucleotide-binding sites. *J Biol Chem* 278: 13757–13764**  
Google Scholar: [Author Only](#) [Title Only](#) [Author and Title](#)
- Dwyer LM, Stewart DW (1986) Effect of leaf age and position on net photosynthetic rates in maize (*Zea Mays* L.). *Agric For Meteorol* 37: 29–46**  
Google Scholar: [Author Only](#) [Title Only](#) [Author and Title](#)
- Evans JR, Poorter H (2001) Photosynthetic acclimation of plants to growth irradiance: the relative importance of specific leaf area and nitrogen partitioning in maximizing carbon gain. *Plant Cell Environ* 24: 755–767**  
Google Scholar: [Author Only](#) [Title Only](#) [Author and Title](#)
- Fox J, Weisberg S (2018) *An R Companion to Applied Regression*. SAGE Publications**  
Google Scholar: [Author Only](#) [Title Only](#) [Author and Title](#)
- Furbank RT (2011) Evolution of the C(4) photosynthetic mechanism: are there really three C(4) acid decarboxylation types? *J Exp Bot* 62: 3103–3108**
- Ghannoum O, Evans JR, Chow WS, Andrews TJ, Conroy JP, von Caemmerer S (2005) Faster Rubisco is the key to superior nitrogen-use efficiency in NADP-malic enzyme relative to NAD-malic enzyme C4 grasses. *Plant Physiol* 137: 638–650**  
Google Scholar: [Author Only](#) [Title Only](#) [Author and Title](#)
- Harmer SL, Covington MF, Bläsing O, Stitt M (2018) Circadian regulation of global gene expression and metabolism. *Annual Plant Reviews online* 133–165**  
Google Scholar: [Author Only](#) [Title Only](#) [Author and Title](#)
- Hatch MD, Kagawa T (1976) Photosynthetic activities of isolated bundle sheath cells in relation to differing mechanisms of C-4 pathway photosynthesis. *Arch Biochem Biophys* 175: 39–53**  
Google Scholar: [Author Only](#) [Title Only](#) [Author and Title](#)
- Heinrich P, Kohler C, Ellmann L, Kuerner P, Spang R, Oefner PJ, Dettmer K (2018) Correcting for natural isotope abundance and tracer impurity in MS-, MS/MS- and high-resolution-multiple-tracer-data from stable isotope labeling experiments with IsoCorrector. *Sci Rep* 8: 17910**  
Google Scholar: [Author Only](#) [Title Only](#) [Author and Title](#)
- Hernández-Sebastià C, Marsolais F, Saravitz C, Israel D, Dewey RE, Huber SC (2005) Free amino acid profiles suggest a possible role for asparagine in the control of storage-product accumulation in developing seeds of low-and high-protein soybean lines. *J Exp Bot* 56: 1951–1963**  
Google Scholar: [Author Only](#) [Title Only](#) [Author and Title](#)
- Hikosaka K, Terashima I (1995) A model of the acclimation of photosynthesis in the leaves of C3 plants to sun and shade with respect to nitrogen use. *Plant Cell Environ* 18: 605–618**  
Google Scholar: [Author Only](#) [Title Only](#) [Author and Title](#)
- Kambhampati S, Ajewole E, Marsolais F (2018) Advances in Asparagine Metabolism. In FM Cánovas, U Lüttge, R Matyssek, eds, *Progress in Botany Vol. 79*. Springer International Publishing, Cham, pp 49–74**  
Google Scholar: [Author Only](#) [Title Only](#) [Author and Title](#)
- Kanai R, Edwards GE (1999) The biochemistry of C4 photosynthesis. *C4 plant biology* 49: 87**  
Google Scholar: [Author Only](#) [Title Only](#) [Author and Title](#)
- Khamis S, Lamaze T, Farineau J (1992) Effect of nitrate limitation on the photosynthetically active pools of aspartate and malate in maize, a NADP malic enzyme C 4 plant. *Physiol Plant* 85: 223–229**  
Google Scholar: [Author Only](#) [Title Only](#) [Author and Title](#)
- Lea PJ, Azevedo RA (2007) Nitrogen use efficiency. 2. Amino acid metabolism. *Ann Appl Biol* 151: 269–275**  
Google Scholar: [Author Only](#) [Title Only](#) [Author and Title](#)
- Lin F, Jiang L, Liu Y, Lv Y, Dai H, Zhao H (2014) Genome-wide identification of housekeeping genes in maize. *Plant Mol Biol* 86: 543–554**  
Google Scholar: [Author Only](#) [Title Only](#) [Author and Title](#)
- Lohaus G, Bükler M, Hußmann M, Soave C, Heldt H-W (1998) Transport of amino acids with special emphasis on the synthesis and transport of asparagine in the Illinois Low Protein and Illinois High Protein strains of maize. *Planta* 205: 181–188**  
Google Scholar: [Author Only](#) [Title Only](#) [Author and Title](#)
- Ma F, Jazmin LJ, Young JD, Allen DK (2014) Isotopically nonstationary <sup>13</sup>C flux analysis of changes in *Arabidopsis thaliana* leaf metabolism due to high light acclimation. *Proceedings of the National Academy of Sciences* 111: 16967–16972**  
Google Scholar: [Author Only](#) [Title Only](#) [Author and Title](#)



**Meister M, Agostino A, Hatch MD (1996) The roles of malate and aspartate in C4 photosynthetic metabolism of *Flaveria bidentis* (L.). *Planta* 199: 262–269**

Google Scholar: [Author Only](#) [Title Only](#) [Author and Title](#)

**Niinemets Ü (2016) Leaf age dependent changes in within-canopy variation in leaf functional traits: a meta-analysis. *J Plant Res* 129: 313–338**

Google Scholar: [Author Only](#) [Title Only](#) [Author and Title](#)

**Osorio S, Vallarino JG, Szecowka M, Ufaz S, Tzin V, Angelovici R, Galili G, Fernie AR (2014) Extraction and Measurement the Activities of Cytosolic Phosphoenolpyruvate Carboxykinase (PEPCK) and Plastidic NADP-dependent Malic Enzyme (ME) on Tomato (*Solanum lycopersicum*). *Bio-protocol* 4: e1122–e1122**

Google Scholar: [Author Only](#) [Title Only](#) [Author and Title](#)

**Pandurangan S, Pajak A, Molnar SJ, Cober ER, Dhaubhadel S, Hernández-Sebastià C, Kaiser WM, Nelson RL, Huber SC, Marsolais F (2012) Relationship between asparagine metabolism and protein concentration in soybean seed. *J Exp Bot* 63: 3173–3184**

Google Scholar: [Author Only](#) [Title Only](#) [Author and Title](#)

**Penfield S, Clements S, Bailey KJ, Gilday AD, Leegood RC, Gray JE, Graham IA (2012) Expression and manipulation of phosphoenolpyruvate carboxykinase 1 identifies a role for malate metabolism in stomatal closure. *Plant J* 69: 679–688**

Google Scholar: [Author Only](#) [Title Only](#) [Author and Title](#)

**Pengelly JLL, Sirault XRR, Tazoe Y, Evans JR, Furbank RT, von Caemmerer S (2010) Growth of the C4 dicot *Flaveria bidentis*: photosynthetic acclimation to low light through shifts in leaf anatomy and biochemistry. *J Exp Bot* 61: 4109–4122**

Google Scholar: [Author Only](#) [Title Only](#) [Author and Title](#)

**Pick TR, Bräutigam A, Schlüter U, Denton AK, Colmsee C, Scholz U, Fahnenstich H, Pieruschka R, Rascher U, Sonnewald U, et al (2011) Systems analysis of a maize leaf developmental gradient redefines the current C4 model and provides candidates for regulation. *Plant Cell* 23: 4208–4220**

Google Scholar: [Author Only](#) [Title Only](#) [Author and Title](#)

**Pinto H, Powell JR, Sharwood RE, Tissue DT, Ghannoum O (2016) Variations in nitrogen use efficiency reflect the biochemical subtype while variations in water use efficiency reflect the evolutionary lineage of C4 grasses at inter-glacial CO2. *Plant Cell Environ* 39: 514–526**

Google Scholar: [Author Only](#) [Title Only](#) [Author and Title](#)

**Pinto H, Sharwood RE, Tissue DT, Ghannoum O (2014) Photosynthesis of C3, C3–C4, and C4 grasses at glacial CO2. *J Exp Bot* 65: 3669–3681**

Google Scholar: [Author Only](#) [Title Only](#) [Author and Title](#)

**Pons TL (2016) Regulation of Leaf Traits in Canopy Gradients. In K Hikosaka, Ü Niinemets, NPR Anten, eds, *Canopy Photosynthesis: From Basics to Applications*. Springer Netherlands, Dordrecht, pp 143–168**

Google Scholar: [Author Only](#) [Title Only](#) [Author and Title](#)

**Sage RF, Christin P-A, Edwards EJ (2011) The C(4) plant lineages of planet Earth. *J Exp Bot* 62: 3155–3169**

Google Scholar: [Author Only](#) [Title Only](#) [Author and Title](#)

**Seebauer JR, Moose SP, Fabbri BJ, Crossland LD, Below FE (2004) Amino acid metabolism in maize earshoots. Implications for assimilate preconditioning and nitrogen signaling. *Plant Physiol* 136: 4326–4334**

Google Scholar: [Author Only](#) [Title Only](#) [Author and Title](#)

**Sommer M, Bräutigam A, Weber APM (2012) The dicotyledonous NAD malic enzyme C4 plant *Cleome gynandra* displays age-dependent plasticity of C4 decarboxylation biochemistry. *Plant Biol* 14: 621–629**

Google Scholar: [Author Only](#) [Title Only](#) [Author and Title](#)

**Sonawane BV, Sharwood RE, Whitney S, Ghannoum O (2018) Shade compromises the photosynthetic efficiency of NADP-ME less than that of PEP-CK and NAD-ME C4 grasses. *J Exp Bot* 69: 3053–3068**

Google Scholar: [Author Only](#) [Title Only](#) [Author and Title](#)

**Stelpflug SC, Sekhon RS, Vaillancourt B, Hirsch CN, Buell CR, de Leon N, Kaeppler SM (2016) An Expanded Maize Gene Expression Atlas based on RNA Sequencing and its Use to Explore Root Development. *Plant Genome*. doi: 10.3835/plantgenome2015.04.0025**

Google Scholar: [Author Only](#) [Title Only](#) [Author and Title](#)

**Stitt M, Zhu X-G (2014) The large pools of metabolites involved in intercellular metabolite shuttles in C4 photosynthesis provide enormous flexibility and robustness in a fluctuating light environment. *Plant Cell Environ* 37: 1985–1988**

Google Scholar: [Author Only](#) [Title Only](#) [Author and Title](#)

**Subedi KD, Ma BL (2005) Ear Position, Leaf Area, and Contribution of Individual Leaves to Grain Yield in Conventional and Leafy Maize Hybrids. *Crop Sci* 45: 2246–2257**

Google Scholar: [Author Only](#) [Title Only](#) [Author and Title](#)

**Sugiyama T, Mizuno M, Hayashi M (1984) Partitioning of nitrogen among ribulose-1, 5-bisphosphate carboxylase/oxygenase, phosphoenolpyruvate carboxylase, and pyruvate orthophosphate dikinase as related to biomass productivity in maize seedlings. *Plant Physiol* 75: 665–669**

Google Scholar: [Author Only](#) [Title Only](#) [Author and Title](#)

**Szecowka M, Heise R, Tohge T, Nunes-Nesi A, Vosloh D, Huege J, Feil R, Lunn J, Nikoloski Z, Stitt M, et al (2013) Metabolic fluxes in an illuminated Arabidopsis rosette. *Plant Cell* 25: 694–714**

Google Scholar: [Author Only](#) [Title Only](#) [Author and Title](#)

**Taub DR, Lerdaun MT (2000) Relationship between leaf nitrogen and photosynthetic rate for three NAD-ME and three NADP-ME C4 grasses. *Am J Bot* 87: 412–417**

Google Scholar: [Author Only](#) [Title Only](#) [Author and Title](#)

**Tazoe Y, Noguchi K, Terashima I (2006) Effects of growth light and nitrogen nutrition on the organization of the photosynthetic apparatus in leaves of a C4 plant, *Amaranthus cruentus*. *Plant Cell Environ* 29: 691–700**

Google Scholar: [Author Only](#) [Title Only](#) [Author and Title](#)

**Ubierna N, Sun W, Kramer DM, Cousins AB (2013) The efficiency of C4 photosynthesis under low light conditions in *Zea mays*, *Miscanthus x giganteus* and *Flaveria bidentis*. *Plant Cell Environ* 36: 365–381**

Google Scholar: [Author Only](#) [Title Only](#) [Author and Title](#)

**Walker RP, Acheson RM, Técsi LI, Leegood RC (1997) Phosphoenolpyruvate Carboxykinase in C4 Plants: Its Role and Regulation. *Funct Plant Biol* 24: 459–468**

Google Scholar: [Author Only](#) [Title Only](#) [Author and Title](#)

**Walker RP, Chen ZH, Tecsli LI, Famiani F, Lea PJ, Leegood RC (1999) Phosphoenolpyruvate carboxykinase plays a role in interactions of carbon and nitrogen metabolism during grape seed development. *Planta* 210: 9–18**

Google Scholar: [Author Only](#) [Title Only](#) [Author and Title](#)

**Walters RG (2005) Towards an understanding of photosynthetic acclimation. *J Exp Bot* 56: 435–447**

Google Scholar: [Author Only](#) [Title Only](#) [Author and Title](#)

**Wang Y, Bräutigam A, Weber APM, Zhu X-G (2014) Three distinct biochemical subtypes of C4 photosynthesis? A modelling analysis. *J Exp Bot* 65: 3567–3578**

Google Scholar: [Author Only](#) [Title Only](#) [Author and Title](#)

**Ward DA, Woolhouse HW (1986) Comparative effects of light during growth on the photosynthetic properties of NADP-ME type C4 grasses from open and shaded habitats. II. Photosynthetic enzyme activities and metabolism. *Plant Cell Environ* 9: 271–277**

Google Scholar: [Author Only](#) [Title Only](#) [Author and Title](#)

**Weissmann S, Ma F, Furuyama K, Gierse J, Berg H, Shao Y, Taniguchi M, Allen DK, Brutnell TP (2016) Interactions of C4 Subtype Metabolic Activities and Transport in Maize Are Revealed through the Characterization of DCT2 Mutants. *Plant Cell* 28: 466–484**

Google Scholar: [Author Only](#) [Title Only](#) [Author and Title](#)

**Wingler A, Walker RP, Chen ZH, Leegood RC (1999) Phosphoenolpyruvate carboxykinase is involved in the decarboxylation of aspartate in the bundle sheath of maize. *Plant Physiol* 120: 539–546**

Google Scholar: [Author Only](#) [Title Only](#) [Author and Title](#)